Silver Nanoparticles Deposited Layered Double Hydroxide Nanoporous Coatings with Excellent Antimicrobial Activities

*Chunping Chen, Poernomo Gunawan, Xiong Wen (David) Lou, and Rong Xu**

Simple and facile processes to produce silver nanoparticles deposited layered double hydroxide (Ag-LDH) coatings are reported. High quality nanoporous LDH coatings are obtained under hydrothermal conditions via an improved in situ growth method by immersing the substrates in LDH suspensions after removal of free electrolytes. Different types of substrates including metal, ceramics, and glass with planar and non-planar surfaces can all be coated with the oriented LDH films with strong adhesion. The pore size can be easily tuned by changing the metal:NaOH ratio during the precipiation process of LDH precursors. In the presence of LDH coatings, silver ions can be readily reduced to metallic silver nanoparticles (Ag NPs) in aqueous solutions. The resulting Ag NPs are incorporated evenly on LDH surface. The Ag-LDH coating exhibits excellent and durable antimicrobial activities against both Gram-negative (E. Coli and P. Aeruginosa) and Gram-positive (B. Subtilis and S. Aureus) bacteria. Even at the 4th recycled use, more than 99% of all types of bacteria can be killed. Moreover, the Ag-LDH coating can also effectively inhibit the bacterial growth and prevent the biofilm formation in the nutrient solutions. These newly designed Ag-LDH coatings may offer a promising antimicrobial solution for clinical and environmental applications.

1. Introduction

Despite the great advances achieved in nanomaterials fabrication, generation of high quality functional coatings from nanomaterials by simple processes remains an important task in order to widen the applications of nanomaterials. Layered double hydroxides (LDHs), owing to their interesting properties in compositional flexibility, anion exchangeability and biocompatibility, have attracted great attentions in many technologically important fields such as catalysis,[1] separation,[2,3] biomedicine.[4–7] LDHs have been demonstrated as promising inorganic building blocks towards the generation of films and coatings for anti-corrosion, sensing, electrochemical and optical applications, etc.[8–18] In recent years much attention has been paid on the development of antimicrobial surfaces for medical devices, household products, food packaging, etc., due to an escalating pressure exerted by the disease-causing microbes on the public health.[19,20] Inorganic coatings which exhibit good mechanical strength, chemical stability, and physicochemical compatibility with ceramic and metallic objects are of particular interest for antimicrobial applications.[21,22] To the best of our knowledge, LDHs-coated surfaces with antimicrobial functionality have not been reported so far.

In this work, we developed i) an improved in situ growth method to generate high-quality nanoporous LDH coatings and ii) a simple process for the deposition of silver nanoparticles on LDH coatings. In the commonly adopted in situ growth process by others, the substrates which may also be the metal sources are first placed in the reaction bath. The LDH crystals formed by co-precipitation using urea or ammonia precipitants then grow as oriented films on the substrates.[8–12] Certain limitations of this method have been reported in these studies which include: i) slow precipitation is necessary to grow high quality film; ii) when urea hydrolysis is adopted, generally only Mg/Al-LDH films can be formed excepted the work by Li et al. in which Ni/Al-LDH film was generated on the surface of Ti foil;[12] iii) when ammonia is used, only metals can be used as the substrates. In contrast to the conventional method, we adopted a convenient rapid co-precipitation process using NaOH precipitant for the preparation of LDH seeds. The seeds separated from the mother liquor were re-dispersed in the deionized water and subsequently the LDH coatings were developed at the crystal growth stage under hydrothermal conditions. This simple process allowed us to fabricate LDH coatings of high quality as well as controllable pore size on various substrates including metal, ceramics, and glass of planar and non-planar surface. Other than Mg/Al-LDH, Ni/Al-LDH coating on Ti substrate can also be produced.

Colloidal silver or silver ions have been demonstrated as effective biocidal agents against a wide range of bacteria based on several mechanisms of protein/DNA damaging, disrupting electron transport pathway and cell wall collapsing.[23–28] Silver incorporated antimicrobial inorganic coatings of titanium oxide[29] and zeolite[30] have been demonstrated with good antimicrobial properties. Recently, Carja et al. reported that silver nanoparticles can be generated on the surface of LDH nanoparticles during the reconstruction process of LDH without organic additives. Their interesting Ag-LDH composite presented

C. Chen, Dr. P. Gunawan, Prof. X. W. (David) Lou, Prof. R. Xu
School of Chemical and Biomedical Engineering
Nanyang Technological University
62, Nanyang Drive, 637459, Singapore
E-mail: rxu@ntu.edu.sg

DOI: 10.1002/adfm.201102333

a good opportunity for developing antimicrobial functional anionic clays by a simple process.[31] In the present study, we found that silver nanoparticles (Ag NPs) can be directly deposited on LDH coatings by in situ reduction of Ag^+ ions without the use of any reducing agents. The resultant Ag-LDH coatings exhibited excellent antimicrobial properties against both Gram-positive and Gram-negative bacteria. The simple and facile methods developed in this study offer the good opportunity for fabrication of high quality LDH films and coatings for versatile applications including antimicrobial surfaces.

2. Results and Discussion

2.1. Properties of Mg/Al-LDH Coatings

The SEM image of the Mg/Al-LDH coating formed on the flat glass substrate with a M:OH ratio at 1:3 (in the precursor solutions) is shown in **Figure 1**A. It can be observed that the well oriented and nanoporous coating was formed by the simple procedure we adopted. The coating after hydrothermal treatment for 24 h has a thickness of around 800 nm and two distinct layers can be seen from the cross-sectional SEM image (Figure 1A inset). The lower layer is comprised of densely packed and randomly oriented nanoparticles of about 100 nm in size. The building blocks in the upper layer exhibit a typical platelet-like morphology of LDHs which stand vertically on the top of the dense layer. The lateral sizes of the platelets are in a range of 300–500 nm and their thickness is about 100 nm. A two-stage growth process can be proposed based on such observations. At the beginning, the LDH nanocrystals are attached to the substrate randomly to form the "foundation" and subsequently the oriented film grows on top of it. The larger particle size in the upper layer can be attributed to a continual crystal growth under the hydrothermal conditions by Ostwald ripening process. The SEM image of the sample collected at 4 h of hydrothermal reaction (Figure S1, Supporting Information (SI)) provides the supporting evidence as LDH nanocrystals are deposited randomly on the substrate at this stage. The XRD pattern of the powder scraped from the Mg/Al-LDH coating (**Figure 2**C) shows the characteristic (003) and (006) basal peaks of LDH crystals. However, compared to the pattern of the LDH powder collected from the suspension of the same bath after hydrothermal reaction (Figure 2A), the extra peaks in Figure 2C indicated by the asterisks show that an impurity phase of magnesium aluminum silicate (JCPDS #76-0537) is present. This is expected due to the partial dissolution of the glass substrate in the alkaline condition (pH of the LDH suspension was 10 ~ 11) and Si was incorporated into the coating to form this impurity phase. The measured Mg:Al atomic ratio in the film by ICP is 2.05:1 which coincides within experimental errors with that in the precursor solution.

Our study has revealed that to develop high quality nanoporous LDH coatings using this convenient rapid co-precipitation by NaOH, it is critical to remove the electrolytes in the reaction medium prior to the hydrothermal treatment. As shown in Figure 1B, low-quality and randomly stacked LDH coating was obtained when the glass substrate was directly placed in the mixture after co-precipitation without the steps of washing and re-dispersing the LDH seeds in water (i.e., Na^+ and NO_3^- electrolytes were not removed). To further prove this finding, a control sample prepared by adding an equivalent amount of $NaNO_3$ into the washed and re-dispersed LDH suspension was prepared by keeping other conditions the same. As shown in the SI, Figure S2, the coating obtained is also non-continuous and consists of randomly aggregated particles. Xu et al. discovered that the presence of the salts in the reaction mixture is the major factor that leads to the aggregation of LDH particles in the suspension.[32] Correspondingly, the stable LDH suspension (Figure 1C) provides a good opportunity for individual LDH particles to seed on the surface of the substrate followed by oriented growth to form LDH coatings. In contrast, the agglomerated LDH particles in the suspension formed without the removal of the electrolytes (Figure 1D) fail the formation of high quality coatings.

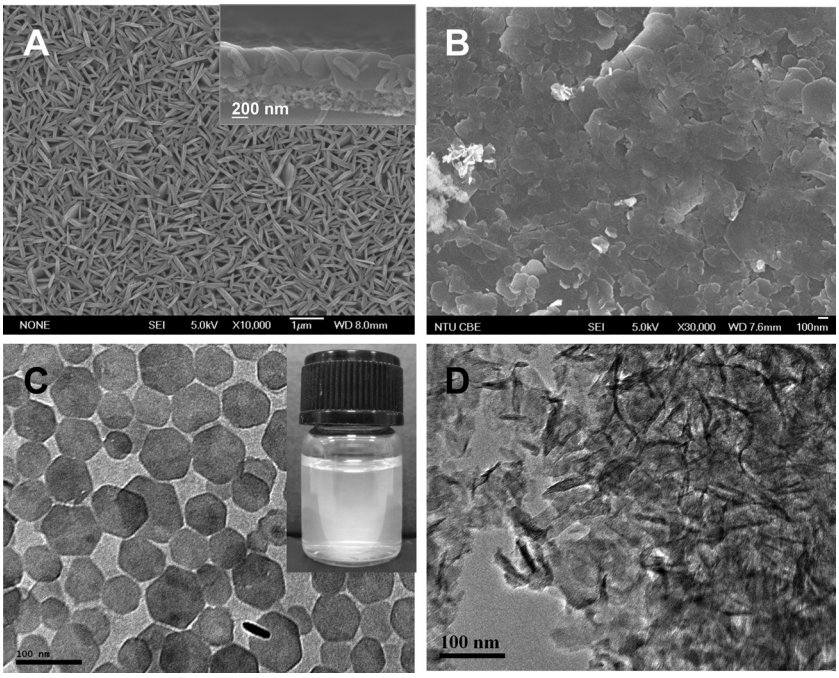

Figure 1. SEM images of the LDH coatings formed on the glass substrate with M:OH ratio at 1:3 under hydrothermal conditions (100 °C for 24 h) with (A) and without (B) removal of the electrolytes from the LDH precursor solutions, and TEM images of their corresponding LDH particles in the suspensions after hydrothermal reaction are shown in (C) and (D), respectively. Inset of A: the cross-sectional image of the coating, and inset of C: the photo of the stable LDH suspension in which high quality LDH coating can be formed.

The textural properties of the coating can be tuned by varying the M:OH ratio. As shown in **Figure 3**A, at the M:OH ratio of 1:2, the coating consisting of large pores was formed with larger and thinner LDH nanosheets. As the M:OH ratio was changed to 1:2.5, 1:3 and 1:4, the LDH nanoplatelets became laterally

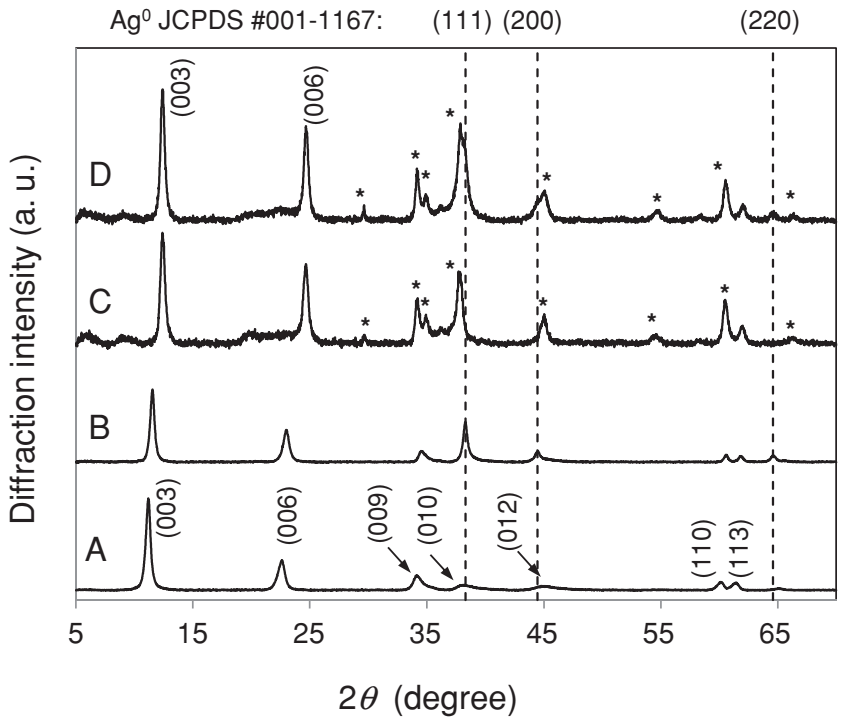

Figure 2. XRD diffraction patterns of (A) LDH powder sample obtained from the suspension, (B) Ag-LDH powder, (C) LDH coating scraped from the glass substrate, and (D) Ag-LDH coating scraped from the glass substrate.

smaller but thicker leading to the formation of denser coatings (Figure 3B–D). Such results can be well associated to the process of nucleation and crystallization. A higher basicity during co-precipitation leads to a larger degree of supersaturation and consequently the formation of more nuclei. This in turn results in generation of smaller particles. In addition, the difference in growth rate along different crystal directions is less obvious at such conditions. Therefore, the aspect ratio of LDH nanoplatelets decreased at higher NaOH concentrations. Similar results have been reported by Liu et al. by varying the concentration of ammonia.[8]

The method developed in this work can also be readily applied with other substrates such as Ti plate (**Figure 4**A) and ceramic plate (Figure 4B) to obtain continuous and oriented coatings. The XRD pattern of LDH coating scraped from Ti plate (not shown) did not show the formation of an analogue phase of magnesium aluminum silicate formed in the case of glass. Some pores sized a few micrometers can be observed in the coating on the ceramic plate. These pores were originated from the ceramic plate itself. Based on our SEM analysis, the surface of the ceramic plate used in this work is

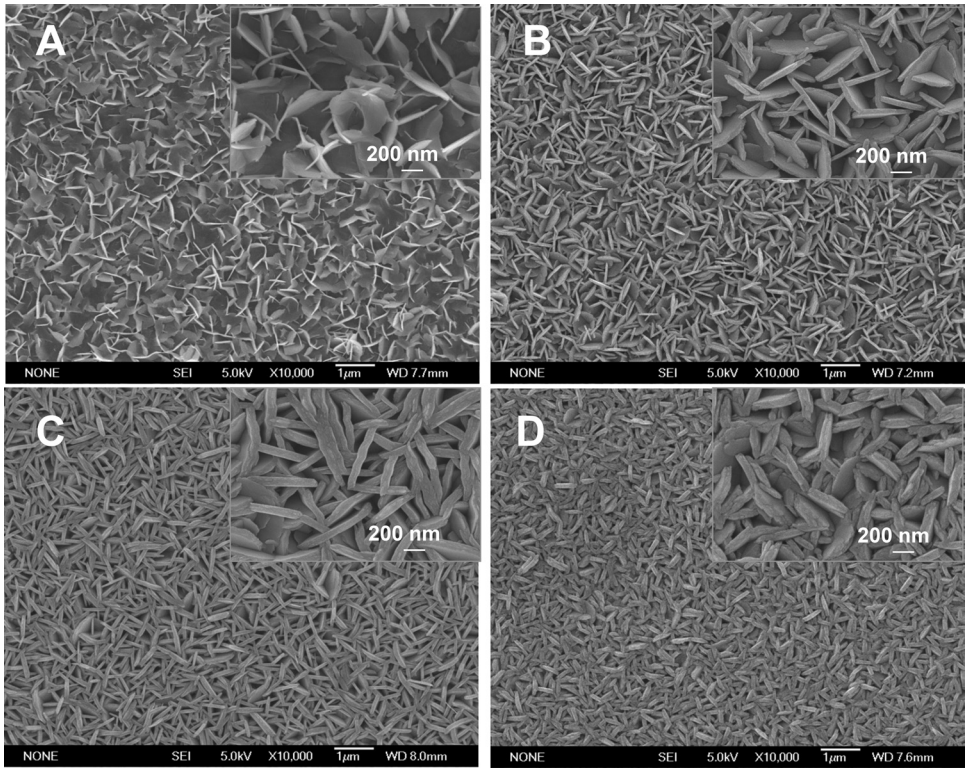

Figure 3. SEM images of LDH coatings formed with different ratios M:OH used during the co-precipitation step, (A) 1:1, (B) 1:2 (C) 1:3, and (D) 1:4 (inset: the images at high magnifications).

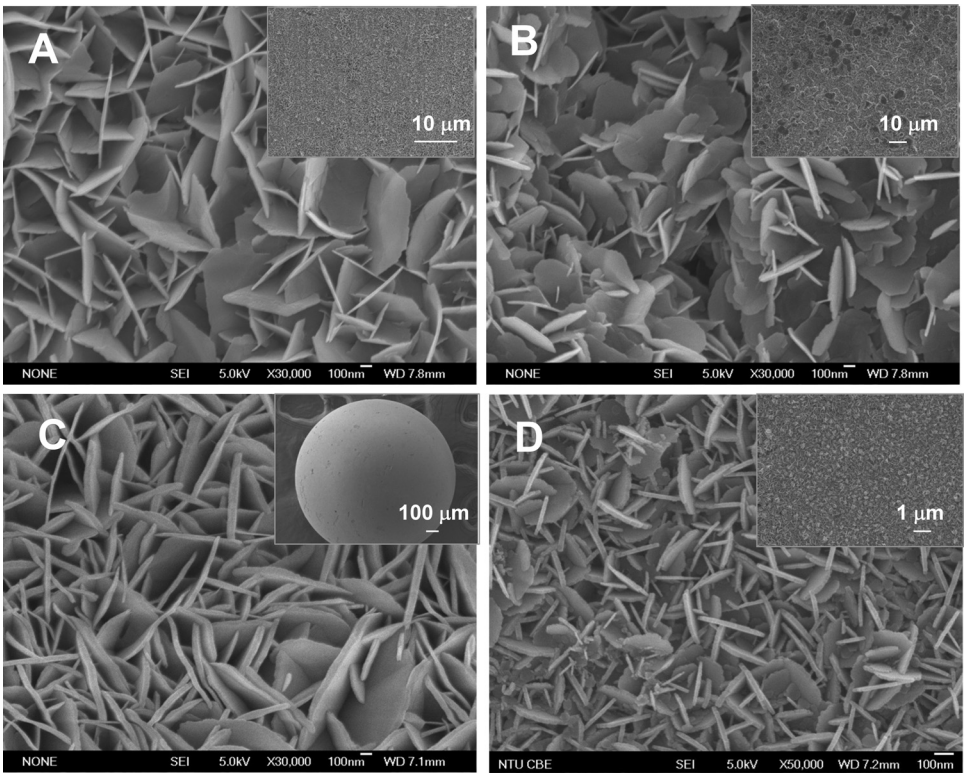

Figure 4. SEM images of Mg/Al-LDH coatings formed on (A) Ti plate, (B) ceramic slide and (C) glass beads, and of (D) Ni/Al-LDH coating formed on Ti plate (inset: the images at low magnifications).

not smooth and consists of micrometer-sized particles with interparticle spaces. As a result, such topological properties were replicated to the morphology of LDH coating. In addition, substrates with a nonplanar surface like glass beads (Figure 4C) can be coated uniformly with the LDH film. Besides Mg/Al-LDH, continuous Ni/Al-LDH coating on Ti plate has also been easily produced by the same method as shown in Figure 4D. In all these cases, a good adhesion of the LDH coatings on the substrates has been attained as the coatings cannot be removed by ultrasonication. As shown in Figure S3A and S3B (Supporting Information), LDH coatings on glass substrate and Ti plate exhibit no obvious changes in morphology and continuity after 2 h of ultrasonication treatment. Furthermore, an adhesion test was conducted for these two samples. According to the plot of the friction response (in terms of relative voltage output) versus the load as shown in Figure S4 (SI), it can be found that the critical load at which total peel-off of the coating from the substrate occurred for LDH coating on glass and Ti substrates was 590 mN and 185 mN, respectively. The stronger adhesion strength between LDH coating and glass substrate should be associated with the presence of magnesium aluminum silicate phase at the interface between LDH coating and glass. Such critical loads are comparable with those reported by others for coatings with strong adhesion on the substrate.[33]

2.2. Characterization of Ag-LDH Coatings

The LDH coating formed with the M:OH ratio of 1:3 on glass substrate (as shown in Figure 1A) was chosen as a model sample for further antimicrobial functionalization. At the first hour after immersion in the $AgNO_3$ solution at 100 °C, the color of the coating turned light grey and further changed to be darker at 3 h. The elemental analysis results provided consistent evidence that the silver content increased with the reaction time and the weight percentage of silver reached around 9.0% (or 7.6 atom% on a metal basis) of the coating after 3 h of reaction. The XRD pattern of the Ag-LDH-3h powder scraped from the glass is shown in Figure 2D. Compared to the pattern of LDH without silver (Figure 2C), extra diffraction peaks appear at the positions indicated by the dotted lines which can be assigned to the (111), (200) and (220) diffractions of cubic phased silver metal (JCPDS #01-1167), although the first two peaks partially overlap with those of the magnesium aluminum silicate impurity phase. The XPS spectra of Ag 3d (**Figure 5**A) further confirmed the formation of silver metal in the coating. Along the reaction time, the signal of Ag 3d peak increased and the peak position of Ag $3d_{5/2}$ was found at binding energy of around 368.2 eV which can be ascribed to metallic silver.[34,35] At 1 h of reaction time, the XPS signal of Ag was quite weak. The TEM image of the powder sample scraped from the coating indicated that Ag NPs of a few nanometers were already formed on the surface of LDH support (Figure S5A, SI). Such small sized nanoparticles cannot be observed in the SEM image (Figure S5B, SI). When the reaction time was extended to 3 h, based on the SEM image shown in Figure 5B, some Ag NPs of about 50 nm are present on the outer surface of the LDH coating. However, the TEM image of the sample scraped from the coating indicates that the majority of the Ag NPs are sized in a range of

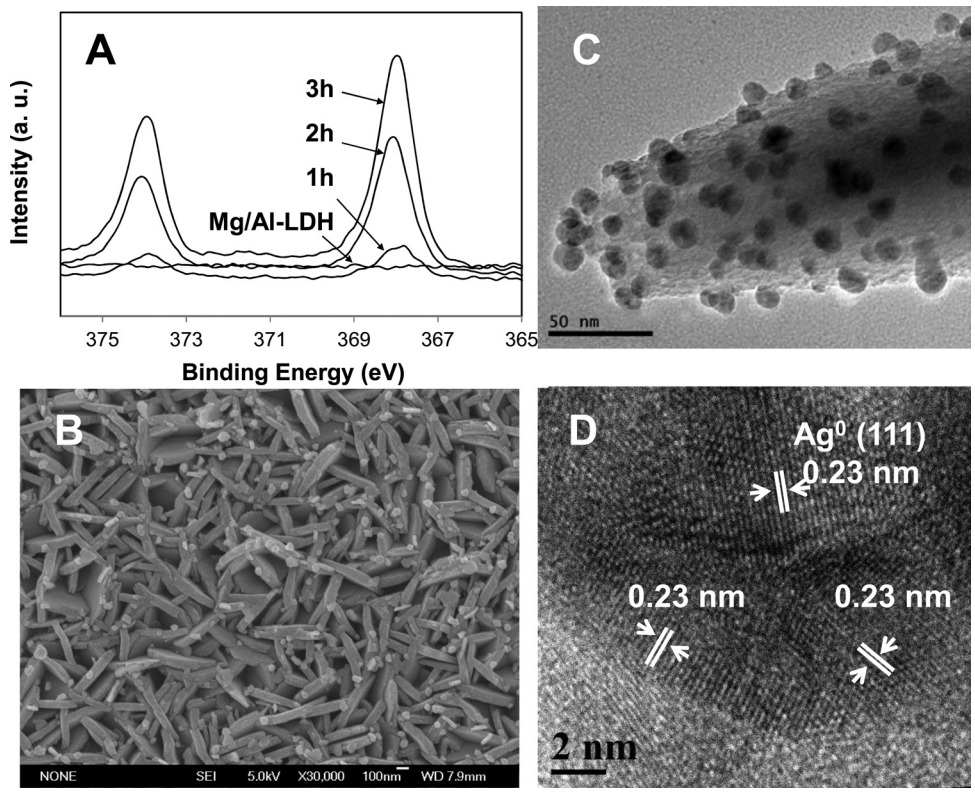

Figure 5. (A) XPS spectra of Ag 3d of LDH coating and Ag-LDH coatings at 1–3 h of reaction time with $AgNO_3$ in aqueous solutions, (B) SEM image of Ag-LDH 3 h coating, (C) and (D) TEM and HRTEM images of Ag-LDH coating scraped from the substrate.

5–20 nm and they are well dispersed on the surface of LDH support (Figure 5C). The formation of larger nanoparticles on the outer surface (i.e., at the solid–liquid interface) is understandable since the outer surface was exposed to the higher concentration of Ag^+ ions. The lattice distance measured in the HRTEM image (Figure 5D) of an individual Ag NP is around 0.23 nm which coincides with (111) *d*-spacing of cubic phased silver metal. Ag NPs deposited LDH powder sample can also been obtained by mixing $AgNO_3$ solution and the LDH suspension under the same conditions. The XRD pattern of Ag-LDH powder in Figure 2B exhibits the typical (111), (200) and (220) diffractions of metallic silver.

Ag NPs have been synthesized extensively by the wet chemical reduction method in the presence of reducing agents.[36] Nishimura et al. have recently elucidated that NaOH accelerates the chemical reduction of Ag^+ ions and nucleation of Ag NPs through the formation of Ag_2O intermediate.[37] The surface of our LDH coating has abundant –OH groups and hence Ag_2O could be formed after Ag^+ ions complexed with the surface –OH groups as shown in Equation 1. Different from the conventional wet chemical reduction method, our process does not require any reducing agent. It is suggested that the self-redox reaction of Ag_2O may occur under the influence of indoor light. Ag_2O is a p-type semiconductor.[38] The photo-generated electrons and holes in Ag_2O may facilitate its redox reaction towards the formation of Ag NPs and oxygen gas, as indicated in Equations 2 and 3.

$$Ag^+ + OH \cdots LDH \rightarrow AgOH \cdots LDH \rightarrow Ag_2O \cdots LDH \quad (1)$$

$$Ag_2O + h\nu \longrightarrow h^+ + e^- \ (h\nu: \text{indoor light}) \quad (2)$$

$$Ag_2O + h + e^- \rightarrow Ag + O_2 \quad (3)$$

The formation of Ag NPs can also be verified by the surface plasmon resonance band at around 400 nm measured by the UV–vis spectroscopy (Figure S6, SI). The larger Ag NPs in the sample after 3 h of reaction lead to a broadened and slightly red-shifted plasmon band.[39]

2.3. Antimicrobial Performances of Ag-LDH Coatings

The biocidal efficacy of the Ag-LDH coatings on the glass substrate was investigated by a colony-counting method for both Gram-negative (*E. coli* and *P. aeruginosa*) and Gram-positive (*S. aureus* and *B. substilis*) bacteria. Both the glass substrate (control) and the LDH coating without Ag NPs did not show any antimicrobial activities. The Ag-LDH coating exhibited excellent activities against all bacteria tested. In all the tests, 100% of bacteria were killed after 3 h incubation in the PBS solution containing the Ag-LDH coated glass substrates with a silver dosage of around 8 μg mL^{-1}. Moreover, a good stability of our Ag-LDH coating is attained as demonstrated by the recycle runs (**Figure 6**). At the 4th consecutive test, the kill percentages of

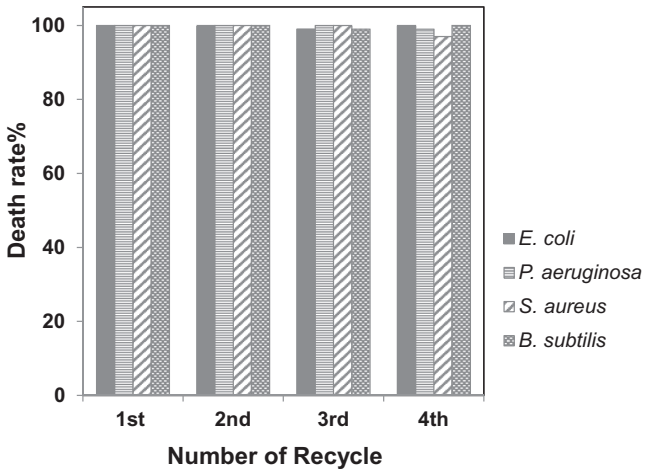

Figure 6. The biocidal efficacy of the Ag-LDH 3h coating on the glass substrate against *E. coli, P. aeruginosa, S. aureus and B. subtilis.*

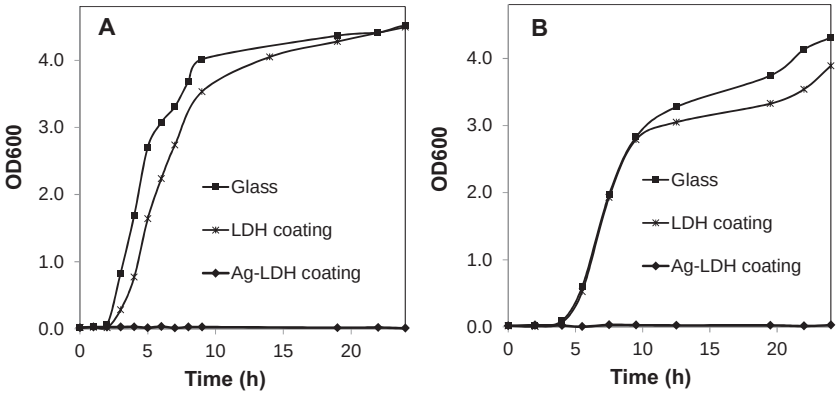

Figure 7. Bacterial growth curves of (A) *E. coli* and(B) *B. subtilis* in LB broth in the presence of the glass substrate, LDH coating and Ag-LDH coating on the glass substrates.

in the LB broth medium. The growth of bacteria was monitored by the optical density at 600 nm (OD_{600}). As shown in **Figure 7**, the glass substrate and LDH coating alone cannot inhibit the growth of bacteria. However, in the presence of Ag-LDH coating, the growth of both types of bacteria was completed inhibited in 24 h of the culture period. Such efficient and durable performances make our Ag-LDH coatings suitable for repeated or long-term antimicrobial applications.

Bacterial infections by biofilm pathogenes represent one of the most serious health issues in recent years and the development of anti-biofilm surfaces has become an urgently important subject.[40] It has been reported that the formation of biofilm takes place through a few steps including adsorption and irreversible adhesion of bacterial cells to the surface followed by colonization.[41] In this study, the anti-biofilm property of our LDH and Ag-LDH coatings was also investigated. After 24 h culture, living bacterial aggregates of high density can be easily observed on the surface of the control glass (**Figure 8**A). However, only individual bacteria can be found attached on the LDH surface (Figure 8B), indicating that the LDH surface can possibly reduce the adsorption and adhesion of the bacteria and hence retard the biofilm formation. This should be attributed to a higher hydrophilicity of the LDH coating compared with that of the glass surface. As shown in Figure S7 (SI), the contact angles of LDH and glass surfaces were measured to be 11.4° and 22.4°, respectively. Due to the combined effects of biocidal Ag NPs and LDH surface, it is no surprise to find that neither biofilm nor the living cells can be observed on the surface of Ag-LDH coating (Figure 8C). These results suggest that the Ag-LDH coatings prepared in this work are able to prevent the biofilm contamination in addition to killing the planktonic bacteria.

the bacteria were still as high as 100% for *E. coli*, 99% for *P. aeruginosa*, 97% for *S. aureus* and 100% for *B. substilis*. The LDH coating was found strong enough to withstand such test. After 4 runs, there was no obvious change in the morphology of the coating as shown in Figure S3D (SI). Based on the ICP measurement, 74% of silver was still remained in the coating after being used for 4 times. The growth behaviors of *E. coli* and *B. substilis* in the presence of Ag-LDH coating were studied

3. Conclusions

In summary, we have developed a simple method to grow LDH coatings in the homogenous suspension of the LDH precursors after removal of the free electrolytes under the hydrothermal condition. The nanoporous and well oriented LDH coatings with controllable porosity can grow on different substrates such as titanium, ceramics and glass and on both planar

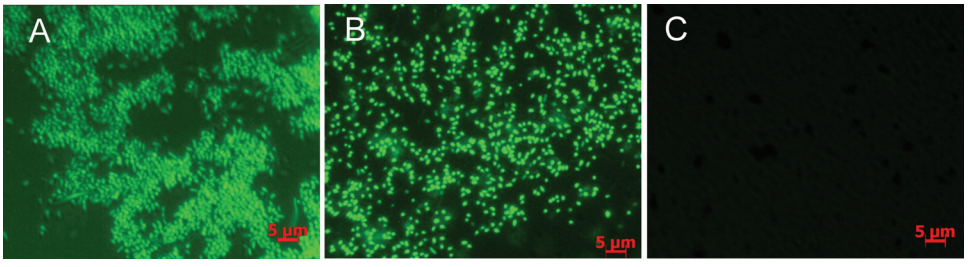

Figure 8. Confocal microscopy images of *E. coli* on the surface of (A) glass, (B) LDH coating, and (C) Ag-LDH coating after 24 h of culture (live cells stained green).

and non-planar surfaces. It was found that the LDH coatings can be readily deposited with silver nanoparticles by directly immersing the coatings in $AgNO_3$ aqueous solution without any additional reducing agents and toxic organic solvents. The resulting Ag-LDH coatings presented excellent antimicrobial activities in killing the planktonic bacteria and biofilm inhibition. It is expected that such low-cost and efficient antimicrobial inorganic coatings could find potential clinical and environmental applications.

4. Experimental Section

Materials and Reagents: Magnesium nitrate hexahydrate ($Mg(NO_3)_2\,6H_2O$, 99%, BDH), Aluminum nitrate nonahydrate ($Al(NO_3)_3\,9H_2O$, 99%, ACROS Organics), NaOH (>99%, pellet, Merck), Silver nitrate ($AgNO_3$), Sodium nitrate ($NaNO_3$, >99%, Sigma-Aldrich). All the substrates including glass slides (25 mm × 25 mm), Ti plates (25 mm ×25 mm), ceramic slides (25 mm ×25 mm) and glass beads (1-2 mm in diameter) were obtained commercially and cleaned with ethanol and water by ultrasonication. The bacterium strains used in this work are *Escherichia coli* (*E. coli*, ATCC8739), *Pseudomonas aeruginosa* (*P. aeruginosa,* ATCC9027), *Bacillus subtilis* (*B. subtilis*, ATCC6051) and *Staphylococcus aureus* (*S. aureus*, ATCC6538).

Synthesis of LDH Coatings: The LDH precursors were first prepard by a method similar to that discribed in our previous work.[3] Briefly, an aqueous solution (10 mL) containing $Mg(NO_3)_2{\cdot}6H_2O$ (512.82 mg, 2.0 mmol) and $Al(NO_3)_3{\cdot}9H_2O$ (375.13 mg, 1.0 mmol) was added quickly into NaOH aqueous solution (40 mL) under vigorous stirring. The molar ratio of total metal ions (Mg^{2+} an Al^{3+}) to NaOH (M:OH) was varied at 1:1, 1:2, 1:3, and 1:4. The mixture was continuously stirred for another 30 min. The precipitate was centrifuged and washed with deionized water twice, and then re-dispersed in deionized water to obtain a 40-mL suspension with a concentration of LDH at 2.33 mg mL^{-1}. The resulting suspension was transferred to a 45-mL Teflon-lined autoclave. The glass substrate was immersed vertically into the suspension and the mixture was then hydrothermally treated at 100 °C for 24 h. The resultant LDH coating was washed with deioinized water and dried in the oven at 60 °C. The suspension after hydrotheremal reaction was also collected by centrifugation and dried for the further characterization and use. Two control samples were synthesized to elucidate the effect of electrolytes on the morphology of the LDH coating. The first was prepared without washing the LDH precursor while keeping other conditions the same. The second was obtained by adding an equivalent amount of $NaNO_3$ (509.94 mg, 6 mmol) after washing and re-dispersing the LDH precursor in deionized water. During the preparation of LDH coatings on other substrates, the same procedure was applied. The M:OH ratio and hydrothermal reaction temperature were kept at 1:3 and 100 °C, respectively. The concentration of LDH precursor in the suspension and the hydrothermal treatment duration were varied as follows: Ti plate: 2.33 mg mL^{-1}, 24 h; ceramic slide: 4.66 mg mL^{-1}, 48 h; and glass bead: 4.66 mg mL^{-1}, 24 h. Finally, Ni/Al-LDH coating was also prepared with the same procedure on Ti plate with the concentration of Ni/Al-LDH precursor at 9.875 mg mL^{-1} and hydrothermal reaction duration of 72 h.

Synthesis of Ag-LDH Coatings: The as-prepared LDH coating was immersed in $AgNO_3$ aqueous solution (20 mL, 0.05 M) and then heated at 100 °C for different durations of 1–3 h. The LDH powder sample collected from the suspension after hydrothermal reaction was also deposited with Ag NPs using the same procedure except under constant stirring.

Characterization: The morphological properties of the coating were observed using field emission scanning electron microscopy (FESEM, JEOL JSM 6700 F). The metal composition was measured by inductively coupled plasma (ICP) optical emission spectroscopy (Perkin Elmer ICP Optima 2000DV). The chemical state of silver was characterized by X-ray photoelectron spectroscopy (XPS, Kratos Analytical, Axis Ultra spectrometer) using a monochromated Al Ka X-ray source (1486.7 eV). The C 1s signal (at 285 eV) was used as the internal standard for calibration of the binding energy. Powders were scraped from the coatings for transmission electron microscopy (TEM, JEOL 3010) and X-ray diffraction (XRD, Bruker D2 Diffractometer) analyses. XRD analysis was also carried out for the powder LDH and Ag-LDH samples obtained from the suspension. The surface plasmon resonance spectra of the Ag NPs in the Ag-LDH coating were obtained using UV–vis spectroscopy (Shimadzu UV2450). The contact angle of the glass and LDH coated glass was measured by the sessile drop technique using a FTA200 Dynamic Contact Angle Analyzer. To evaluate the adhesion strength between LDH coating and the substrate, a scratch test was conducted using a scanning scratch tester (SHIMADZU, SST-101) according the method described in the literature.[33] The load at which total peeling-off of the coating from the substrate occurred was used to evaluate the coating/substrate adhesion.

Antimicrobial Performance Test: Antimicrobial test was conducted according to the procedure described in our earlier report.[42] *E. coli* and *P. aeruginosa* were chosen as models of Gram-negative bacteria, and *B. subtilis* and *S. aureus* were selected as models of Gram-positive bacteria. All the target bacteria were cultured to a mid-log phase in Luria-Bertani (LB) broth at 37 °C. The cells were harvested by centrifugation, washed with phosphate buffer saline (PBS, pH = 7.2) and re-suspended in PBS with the cell concentration approximately at 10^5 colony forming units (CFUs) per mL. LDH and Ag-LDH coatings and the glass substrate (control) were immersed in the cell suspensions (16 mL). The mixture was incubated at 37 °C with a gentle shaking at 220 rpm. After 3 h of incubation, the number of viable cells were determined by the colony counting method. The kill percentage of bacteria was calculated by $(N_{control} - N_{sample})/N_{control} \times 100\%$, where $N_{control}$ and N_{sample} represent the number of viable cells in the cell suspensions with control and the sample, respectively. The cell counts before and after the test in the case of control were almost the same, indicating that the glass substrate has no antimicrobial effect. To evaluate the durability of Ag-LDH coating, the sample was reused for the antimicrobial efficacy test under the same conditions for three times. The sample after each test was washed with both sterilized distilled water and PBS twice.

Growth Inhibition Study: The bacteria (*E. coli* and *B. substilis*) were cultured to a mid-log phase in LB broth and re-dispersed in LB broth (16 mL) after washing to obtain a concentration of 10^5 CFUs mL^{-1}. The samples were then immersed in the suspension of bacteria and incubated at 37 °C with shaking at 220 rpm. The growth behavior of bacteria was monitored by measuring the optical density at 600 nm (OD_{600}) based on the turbidity of the suspension using UV-vis spectroscopy (Shimadzu UV2450).

Anti-Biofilm Test: *E. coli* in the mid-log phase was dispersed in LB broth at 10^5 CFUs per mL. Each sample (12.5 mm × 12.5 mm) was placed diagonally into 24-well plate which contained the cell suspension (1.5 mL). The suspension in the plate was cultured at 37 °C with shaking at 100 rpm. After 24 h culture, the samples were washed gently with PBS and stained with SYTO 9 dye. After being incubated in the dark for 15 min at room temperature, the samples were observed under a confocal microscope (Zeiss Axio Scope A1).

Supporting Information

Supporting Information is available from the Wiley Online Library or from the author.

Acknowledgements

This work was supported by AcRF grants (RG4/04 and RG30/07) from Ministry of Education, Singapore. We thank Prof. Matthew Chang, Dr. Huamao Du and Dr. Hua Lin for their assistance with antimicrobial

tests; and Dr. Yongsheng Wang for adhesion test. CP Chen acknowledges the research scholarship from Nanyang Technological University.

Received: September 29, 2011
Revised: October 30, 2011
Published online: December 13, 2011

[1] H. M. Shi, J. He, *J. Catal.* **2011**, *279*, 155.
[2] Y. W. You, H. T. Zhao, G. F. Vance, *Environ. Technol.* **2001**, *22*, 1447.
[3] C. Chen, P. Gunawan, R. Xu, *J. Mater. Chem.* **2010**, *21*, 1218.
[4] P. Gunawan, R. Xu, *Chem. Mater.* **2009**, *21*, 781.
[5] Z. Gu, B. E. Rolfe, Z. P. Xu, A. C. Thomas, J. H. Campbell, G. Q. M. Lu, *Biomaterials* **2010**, *31*, 5455.
[6] J. M. Oh, S. J. Choi, G. E. Lee, S. H. Han, J. H. Choy, *Adv. Funct. Mater.* **2009**, *19*, 1617.
[7] J. H. Choy, J. M. Oh, M. Park, K. M. Sohn, J. W. Kim, *Adv. Mater.* **2004**, *16*, 1181.
[8] J. Liu, Y. Li, X. Huang, G. Li, Z. Li, *Adv. Funct. Mater.* **2008**, *18*, 1448.
[9] F. Zhang, L. Zhao, H. Chen, S. Xu, D. G. Evans, X. Duan, *Angew. Chem. Int. Ed.* **2008**, *47*, 2466.
[10] H. Chen, F. Zhang, S. Fu, X. Duan, *Adv. Mater.* **2006**, *18*, 3089.
[11] J. K. Lin, J. Y. Uan, C. P. Wu, H. H. Huang, *J. Mater. Chem.* **2011**, *21*, 5011.
[12] X. Li, J. P. Liu, X. X. Ji, J. A. Jiang, R. M. Ding, Y. Y. Hu, A. Z. Hu, X. T. Huang, *Sens. Actuator B Chem.* **2010**, *147*, 241.
[13] D. Yan, J. Lu, M. Wei, S. Qin, L. Chen, S. Zhang, D. G. Evans, X. Duan, *Adv. Funct. Mater.* **2011**, *21*, 2497.
[14] D. P. Yan, J. Lu, M. Wei, J. B. Han, J. Ma, F. Li, D. G. Evans, X. Duan, *Angew. Chem. Int. Ed.* **2009**, *48*, 3073.
[15] J. H. Lee, S. W. Rhee, H. J. Nam, D. Y. Jung, *Adv. Mater.* **2009**, *21*, 546.
[16] X. X. Guo, F. Z. Zhang, D. G. Evans, X. Duan, *Chem. Commun.* **2010**, *46*, 5197.
[17] D. P. Yan, J. Lu, J. Ma, M. Wei, D. G. Evans, X. Duan, *Angew. Chem. Int. Ed.* **2010**, *50*, 720.
[18] H. B. Yao, H. Y. Fang, Z. H. Tan, L. H. Wu, S. H. Yu, *Angew. Chem. Int. Ed.* **2010**, *49*, 2140.
[19] I. Banerjee, R. C. Pangule, R. S. Kane, *Adv. Mater.* **2011**, *23*, 690.
[20] S. A. Onaizi, S. S. J. Leong, *Biotechnol. Adv.* **2011**, *29*, 67.
[21] K. Vasilev, J. Cook, H. J. Griesser, *Expert Rev. Med. Devices* **2009**, *6*, 553.
[22] A. Simchi, E. Tamjid, F. Pishbin, A. R. Boccaccini, *Nanomed. Nanotechnol. Biol. Med.* **2011**, *7*, 22.
[23] J. T. Trevors, *Enzyme Microb. Tech.* **1987**, *9*, 331.
[24] A. D. Russell, W. B. Hugo, *Prog. Med. Chem.* **1994**, *31*, 351.
[25] Q. L. Feng, J. Wu, G. Q. Chen, F. Z. Cui, T. N. Kim, J. O. Kim, *J. Biomed. Mater. Res.* **2000**, *52*, 662.
[26] A. Panacek, L. Kvitek, R. Prucek, M. Kolar, R. Vecerova, N. Pizurova, V. K. Sharma, T. Nevecna, R. Zboril, *J. Phys. Chem. B* **2006**, *110*, 16248.
[27] I. Sondi, B. Salopek-Sondi, *J. Colloid Interface Sci.* **2004**, *275*, 177.
[28] M. Lv, S. Su, Y. He, Q. Huang, W. B. Hu, D. Li, C. H. Fan, S. T. Lee, *Adv. Mater.* **2010**, *22*, 5463.
[29] Q. Zhang, C. Sun, Y. Zhao, S. Zhou, X. Hu, P. Chen, *Environ. Sci. Technol.* **2010**, *44*, 8270.
[30] A. M. P. McDonnell, D. Beving, A. J. Wang, W. Chen, Y. S. Yan, *Adv. Funct. Mater.* **2005**, *15*, 336.
[31] G. Carja, Y. Kameshima, A. Nakajima, C. Dranca, K. Okada, *Int. J. Antimicrob. Agents* **2009**, *34*, 534.
[32] Z. P. Xu, G. S. Stevenson, C. Q. Lu, G. Q. Lu, P. F. Bartlett, P. P. Gray, *J. Am. Chem. Soc.* **2005**, *128*, 36.
[33] S. Zhang, X. T. Zeng, Y. S. Wang, K. Cheng, W. J. Weng, *Surf. Coat. Tech.* **2006**, *200*, 6350.
[34] J. F. Moulder, W. F. Stickle, P. E. Sobol, K. D. Bomben, *Handbook of X-ray photoelectron spectroscopy*, Perkin-Elmer, Minnesota, USA**1992**, p. 213.
[35] A. M. Ferraria, S. Boufi, N. Battaglini, A. M. B. do Rego, M. ReiVilar, *Langmuir* **2010**, *26*, 1996.
[36] B. Wiley, Y. Sun, Y. Xia, *Acc. Chem. Res.* **2007**, *40*, 1067.
[37] S. Nishimura, D. Mott, A. Takagaki, S. Maenosono, K. Ebitani, *Phys. Chem. Chem. Phys.* **2011**, *13*, 9335.
[38] R. A. Ismail, K. Z. Yahya, O. A. Abdulrazaq, *Surf. Rev. Lett.* **2005**, *12*, 299.
[39] P. D. Cozzoli, R. Comparelli, E. Fanizza, M. L. Curri, A. Agostiano, D. Laub, *J. Am. Chem. Soc.* **2004**, *126*, 3868.
[40] D. Davies, *Nature Rev. Drug Discovery* **2003**, *2*, 114.
[41] R. Kolter, E. P. Greenberg, *Nature* **2006**, *441*, 300.
[42] W. Yuan, G. H. Jiang, J. F. Che, X. B. Qi, R. Xu, M. W. Chang, Y. Chen, S. Y. Lim, J. Dai, M. B. Chan-Park, *J. Phys. Chem. C* **2008**, *112*, 18754.